ONERA

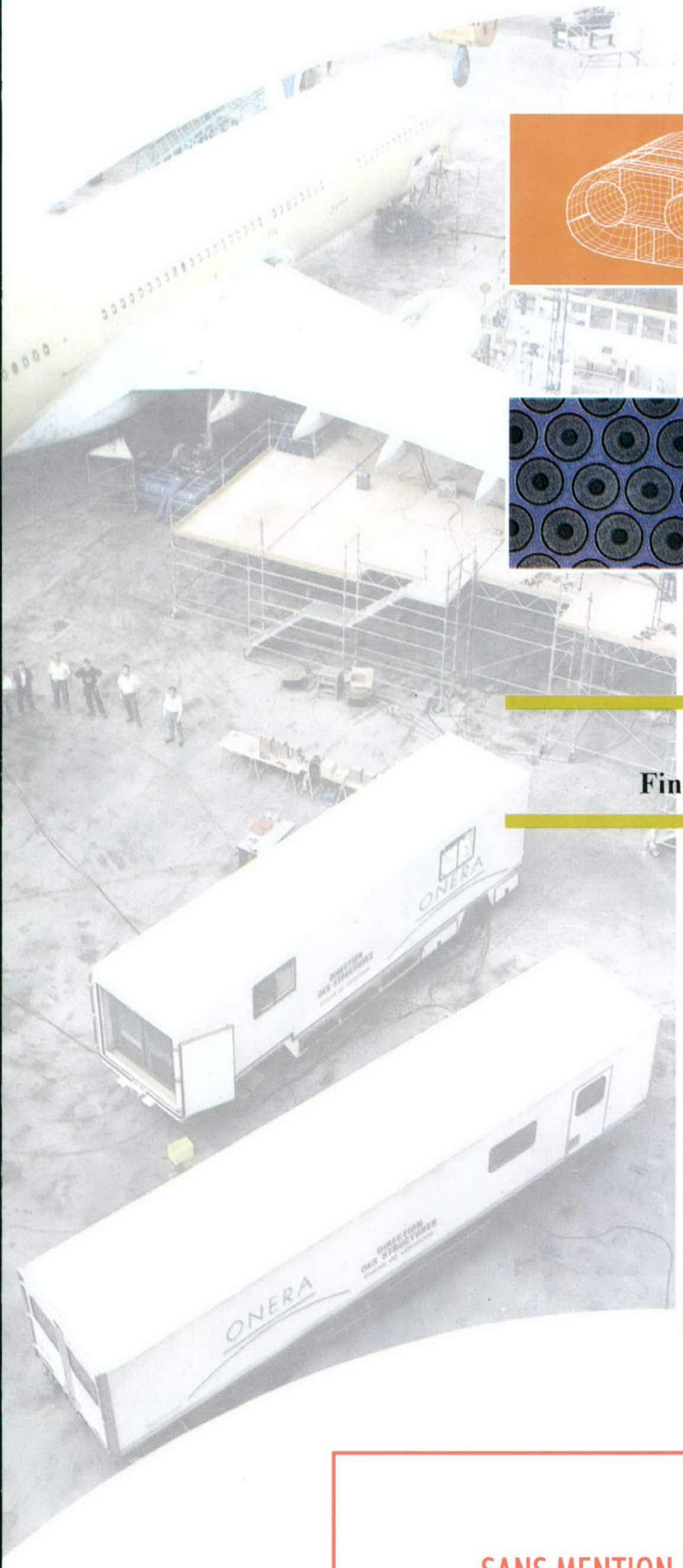

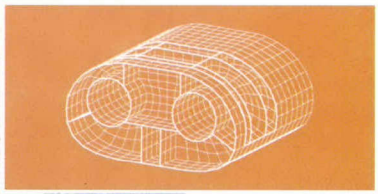

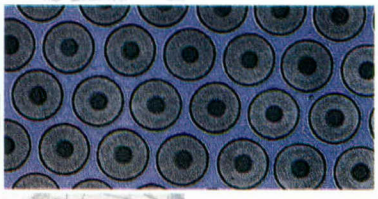

METALLIC MATERIALS AND PROCESSES DEPARTMENT

Final Report

Design and optimization of new metallic materials (metal foams)for the reduction of the noise of the aeronautical turbo engines.

RF 1/06379 DMMP - February 2005

F. Paun ; J. Nadler ; S. Gasser ; P. Josso

MATERIALS AND STRUCTURES

ONERA

BP 72 - 29, avenue de la Division Leclerc
92322 Châtillon Cedex - FRANCE
Tél. : 01 46 73 40 40 - Fax : 01 46 73 41 41
Office National d'Études et de Recherches Aérospatiales

METALLIC MATERIALS AND PROCESSES DEPARTMENT

Final Report N° RF 1/06379 DMMP

February 2005

Design and optimization of new metallic materials (metal foams)for the reduction of the noise of the aeronautical turbo engines.

Written by :
F. Paun ; J. Nadler ; S. Gasser ; P. Josso

This material is based upon work supported by the
Defense Advanced Research Projects Agency
Defense Sciences Office
DARPA Order No. L993/00
Issued by DARPA/CMO under Contract #MDA972-01-C-0075

Approved by :
Head of
Metallic Materials and Processes Department
S. Naka

This document comprises 36 pages

"Any opinions, findings and conclusions or recommendations expressed in this material are those of the authors and should not be interpreted as representing the official policies, either expressly or implied, of the Defense Advanced Research Projects Agency or the U.S. Government."

SMP

IDENTIFICATION CARD of ONERA REPORT N° RF 1/06379 DMMP

Issued by : **METALLIC MATERIALS AND PROCESSES DEPARTMENT**	Contracting Agency : **DARPA**	Contract Number : **MDA972-01C-0075 + AMENDMENT P00004**
	Programme card number:	Date : **February 2005**
Title :**Design and optimization of new metallic materials (metal foams)for the reduction of the noise of the aeronautical turbo engines.**		
Author(s) : **F. Paun ; J. Nadler ; S. Gasser ; P. Josso**		
SECURITY CLASSIFICATION : Civile Title : SANS MENTION DE PROTECTION ID Card : SANS MENTION DE PROTECTION Report : SANS MENTION DE PROTECTION		Timing Classification Off Title : Sans objet ID Card : Sans objet Report : Sans objet

Abstract :
The need to control noise generated by aircrafts has become a major concern for the aeronautic community (both industry as well as civil and military authorities). In order to reduce engine noise, there are two possible approaches: either the reduction in the generation of the noise or the increase in the capacities for absorption of the noise generated. The first approach consists in optimizing the geometry of the exhaust nozzle, an approach which will quickly result in trying to optimally balance performance of an engine and the extent of noise reduction (reduction of the velocity and temperature of the reaction jet gases and increased dispersion of the jet). The present project has explored the second strategy – noise absorption.
The main purpose of this project was to propose a new type of material architecture (microstructure) usable in manufacturing exhaust nozzles with good acoustic absorption capacities by maintaining their overall weight and high temperature mechanical performance.
Since the requirements for thermal loadings are more stringent at the exhaust nozzle level than for mechanical loadings, metal foams appear most to be the appropriate material system for noise reduction. Finding the best solution in terms balancing structural strength and acoustic properties was the main thrust of this project. Acoustic phenomena such as absorption, reflection and transmission and mechanics of Hollow Spheres-based cellular materials were studied and the understanding gained thus far will help engineers designing optimized exhaust nozzles of turbo-engines (high-level loading conditions under pressure and temperature). A method of optimized design was also proposed and tested on a specific study case.
The present project was conducted using a multidisciplinary approach; knowledge in solid mechanics, acoustics, fluid mechanics and metallurgy were all required.

Key words :
NOISE REDUCTION ; CELLULAR MATERIALS ; HIGH TEMPERATURE ; ACOUSTIC ABSORPTION ; ELASTICITY ; MACROSCOPIC ; YIELD CRITERION ; METALLIC FOAMS.

BP 72 - 29, avenue de la Division Leclerc
92322 Châtillon Cedex - FRANCE
Tél. : 01 46 73 40 40 - Fax : 01 46 73 41 41
Office National d'Études et de Recherches Aérospatiales

ONERA

DISTRIBUTION LIST of ONERA REPORT N°RF 1/06379 DMMP

Distribution of report

- **Outside ONERA :**

DARPA/DSO	Dr. L. Christodoulou	1 ex.
DARPA/DSO	Ms. R. Meade	1 ex.
DARPA/CMO	Ms. A. Tate	1 ex.
NRL	Dr. P. Matic	1 ex.
DARPA/ASBD	Library	1 ex.
DTIC-BCS		2 ex.

- **Inside ONERA :**

DMMPst	DMMP/Arch.	1 ex.
DMMP/DD	S. Naka	1 ex.
DMMP	F. Paun	1 ex.
DMMP	J. Nadler	1 ex.
DMMP	S. Gasser	1 ex.
DMMP	P. Josso	1 ex.
DMMP	M.-P. Bacos	1 ex.
ISP	Documentation (original + document électronique + 1 ex.)	1 ex.

Distribution of identification card only

- **Outside ONERA :**

CEDOCAR		1 ex.

- **Inside ONERA :**

DSG/MAS	T. Khan	1 ex.
Systematic distribution : DSG, DTG, DAI, DAJ, DSAC, les Directeurs de MFE, PHY, MAS, TIS, GMT		10 ex.

BP 72 - 29, avenue de la Division Leclerc
92322 Châtillon Cedex - FRANCE
Tél. : 01 46 73 40 40 - Fax : 01 46 73 41 41
Office National d'Études et de Recherches Aérospatiales

ONERA

CONTENTS

FEVRIER 2005

Design and optimization of new metallic materials (metal foams) for the reduction of the noise of the aeronautical turbo engines

1 - INTRODUCTION

The need to control noise generated by aircrafts has become a major concern for the aeronautic community (both industry as well as civil and military authorities). From the environmental standpoint, inhabitants near airports or air bases desire less and less disturbance while modern airplanes and helicopters, as they become more and more powerful, consequently become more and more noisy. For military forces, sound stealth of their aircraft becomes crucial because increasingly sophisticated and powerful technology has emerged, enabling enemy forces to detect these aircrafts through the noise they generate.

In view of this growing concern of the aeronautic community, we have proposed this present research project which aims to provide some new concepts that may give rise to new technologies to reduce the aircraft noise.

2 - OBJECTIVES AND GENERAL METHODOLOGY

In order to reduce engine noise, there are two possible approaches: either the reduction in the generation of the noise or the increase in the capacities for absorption of the noise generated. The first approach consists in optimizing the geometry of the exhaust nozzle, an approach which will quickly result in trying to optimally balance performance of an engine and the extent of noise reduction (reduction of the velocity and temperature of the reaction jet gases and increased dispersion of the jet). The present project has explored the second strategy – noise absorbtion.

The main purpose of this project was to propose a new type of material architecture (microstructure) usable in manufacturing exhaust nozzles with good acoustic absorption capacities by maintaining their overall weight and high temperature mechanical performance.

Since the requirements for thermal loadings are more stringent at the exhaust nozzle level than for mechanical loadings, metal foams appear most to be the appropriate material system for noise reduction. Finding the best solution in terms balancing structural strength and acoustic properties was the main thrust of this project. Acoustic phenomena such as absorption, reflection and transmission and mechanics of Hollow Spheres-based cellular materials were studied and the understanding gained thus far will help engineers designing optimized exhaust nozzles of turbo-engines (high-level loading conditions under pressure and temperature). A method of optimized design was also proposed and tested on a specific study case.

The present project was conducted using a multidisciplinary approach; knowledge in solid mechanics, acoustics, fluid mechanics and metallurgy were all required.

FEVRIER 2005

3 – TECHNICAL PROBLEMS

3.1. Proposed cellular material

The main idea of this project consists in obtaining for the very first time a new type of noise-absorbing material which is also capable of enduring a high level of thermo-mechanical loading (required for a structural material). Usually, noise-absorbing materials cannot withstand mechanical loading do this is the challenge of our project.

By making a preliminary survey of existing materials which may meet the above requirements, we have determined that metallic foams could be the materials that we are looking for. However, the existing information in the literature indicates that the properties of these materials show a large degree of scattering. Such scattering effectively hinders their use in aeronautics.

We have developed a list of requirements to choose our material:

- the temperatures level of 800 to 1000°C , the possibility of thermal chocks and vibrations occurrences in an aggressive thermo-chemical environment inducing possible corrosion and oxidation necessitated the choice of a Ni based alloy as the bulk material for our cellular structure,

- good acoustic absorptive capacities require the presence of a particular open porosity in side the material,

- reliable mechanical resistance demanded a close cell porosity for our cellular material.

Thus our final choice for the appropriate material which satisfied all of the requirements specific for use in the aeronautic turbo engine exhausters and had good acoustic absorption capacity was a Nickel Hollow Spheres (HS) based cellular material, regularly packed in a Face Centered Cubic (FCC) network.

3.2. Processing

The first acoustic test specimens were small steel spheres provided by the bearing industry. At that time, these type of specimens were sufficient for investigating acoustic absorption under the assumption that only the absorption mechanism was viscous fluid dissipation inside the interstitial channels was significant.

We have tested three types of assembling process for joining the steel spheres:

Electrical discharge welding using energies up to 30 KJ was attempted. We have not completely this technique but we still seek out a company owning electrical equipment which would control not only the energy level but also the discharge time. The sintering did not provide definitive results. We tested sintering processes using our laboratory furnaces. The low atmosphere furnace is limited to 1200 K and the resulting welded joints were not strong enough. The hydrogen atmosphere furnace could be used up to 1300 k but did not sufficiently sinter the joints. Our satisfactory solution was brazing. We used a Ni-P chemical deposit and the low atmosphere furnace at 1200 K. The obtained material was cut by electro-discharge machine to provide the acoustic test specimens. In conclusion, brazing seemed to be the most promising way to process these specimens.

FEVRIER 2005

We have further concentrated our efforts in obtaining cellular material presenting an FCC network of hollow spheres made of nickel. The same brazing method was applied to assemble the hollow Ni spheres.

We used the classic Ni-P deposit [1] with a thickness of 5µm on 3 mm diameter spheres. After 20 minutes at 920 C° in a vacuum furnace, we obtained the desired cellular material. We encountered some difficulties due to irregularity in Ni hollow spheres consisting of holes in the walls. During brazing, the Ni-P liquid solution penetrated the spheres and soon liquefied them. Unfortunately, all the test specimens that we tried to obtain in this manner were unusable. At least one sphere in four was totally destroyed in this manner. It is suggested that the Ni-P can disolve many of the hollow sphere walls.

Further investigations including analyzing the hollow spheres before Ni-P deposition, after the Ni-P deposition and after brazing that the original hollow spheres were not hermetic. Statistics show that 90% of hollow spheres were not hermetic before the Ni-P deposition.

This could be explained by one particular stage of the processing. The Ni-P deposit is obtained on the surface of an original polystyrene ball [1]. After a sufficient growth of the Ni deposit, the manufacturer stopped the electro-chemical process and heat treated the balls at 900°C in a vacuum furnace. This exposure pyrolyzed the polystyrene ball and we anticipated that the gasseous products would diffuse throught the Ni hollow sphere wall via micron-scale porosity. However, this didn't happen. As mentioned, 90% of the hollow spheres were permeable, which was easily observed with microscopic investigations.

Thus, the Ni-P, deposited on these permeable Ni hollow spheres, penetrated inside the hollow spheres through the holes as a liquid and the weakest spheres were then destroyed their neighbors during the brazing process.

As a solution, we have modified the initial hollow sphere processing. We have proceeded to the polystyrene elimination and then we restarted de Ni deposit for 40 microns of additional thickness. On these hermetic hollow spheres we made the Ni-P deposit and we obtained reliable test specimens by standard brazing.

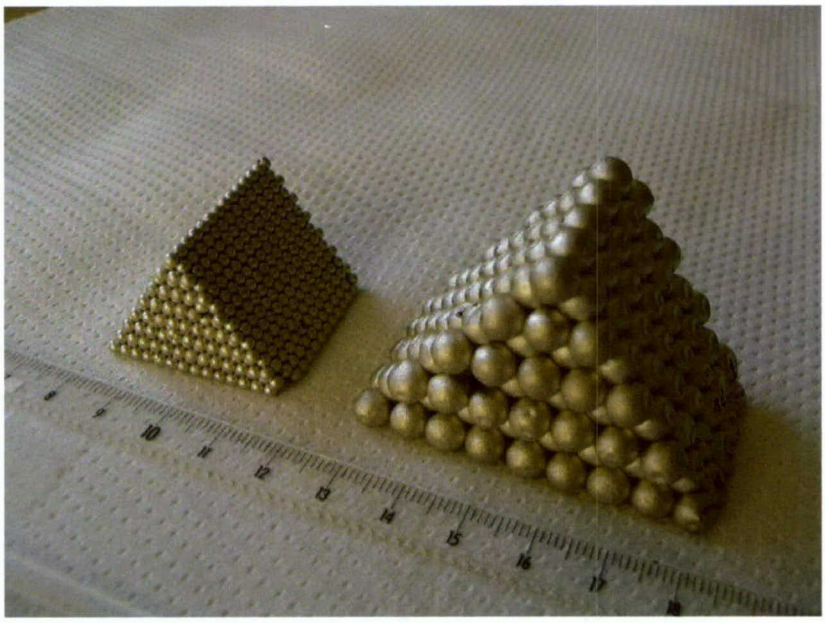

Figure 1 - Test specimens obtained by brazing with NiP Ni Hollow Spheres in an FCC network

FEVRIER 2005

4 – TECHNICAL RESULTS

4.1. Acoustics

4.1.1. Acoustics behavior

The key to understanding the acoustic behavior is a good comprehension of all the possible acoustic absorption mechanisms. Among these, we have already investigated the threee most important.

1) Acoustic absorption due to the small open holes in the walls of hollow sphere. Microscopic observations showed that there were no such holes through these walls. Indeed, the porosity generally present in the Ni electro-chemical deposit does not percolate and gases can not communicate from the inner side of the hollow sphere to the exterior. But first degree approximations* demonstrate that if holes with diameter greater than 10 micrometers appears on the sphere's wall a dissipative process will occur. Calculating this dissipation can not be done by simple analytical approach, so numerical simulation will be necessary. As reported in the processing section we can now obtain improved test specimens containing only hermetic spheres. This absorption mechanisms will thus not be considered.

**Done for 170 dB acoustic intensity and a Poiseuil flow into the hole was admitted.*

2) Intrinsic metallic dissipation. In the case of plastic deformation or some special alloys as Ni-Ru a metallic dissipation could appear. In our case, taking into account a sphere of 1 mm diameter with 10 micrometers thickness of the wall loaded by a pressure corresponding to 170 dB, we obtain no more than 0.006 % of relative deformation. We could thus conclude that there is neither risk of plastic deformation nor that of significant metallic dissipation. The question of special alloys remains still open. Bibliographic investigations will continue concerning this subject.

3) Acoustic absorption by intersphere acoustic flowing. According to our first estimations, the acoustic absorption capacities of our proposed material are based essentially on this mechanism. An exhuastive survey of the current literature was performed. Definitely, the best way to solve our problem is the use of porous media models.

4.1.2. Phenomenological approach

The large majority of these approaches are based on the Kirchoff approach completed by Allard [2]. They made a simplified hypothesis. Openly porous materials are reduced to a network of tubes. Working in this tubular assumption allowed a good description of all the equations. So the wave propagation equation is transformed as follow:

$$\frac{\partial^2 p}{\partial z^2} - \frac{1}{\tilde{c}^2}\frac{\partial^2 p}{\partial t^2} = 0$$

where - $\tilde{c}^2 = \dfrac{\tilde{\gamma}_{eff}}{\tilde{\rho}_{eff}} P_0$, $\tilde{c}$ is a complex number celerity and

P_0 - initial steady pressure,

$\gamma_{eff}, \rho_{eff} = f(\gamma, \rho, \mu, c_p, K, I_1, I_0)$ with:

$\gamma, \rho, \mu, c_p, K$ - gas properties respectively specific heat ratio, density, dynamic viscosity, specific heat and thermal conductivity,

I_1, I_0 - Bessel functions.

We easily deduce the linear acoustic absorption coefficient:

$$\beta = 2\pi\nu \frac{\Im(\tilde{c})}{|\tilde{c}|^2}$$ were ν is the frequency.

This model had to be adapted to our material. In fact, Allard [2] and especially Stinson [3] have already proposed an evolution of tubular model to porous media. They introduced parameters as porosity, tortuosity, and effective radius.

This model seems to provide good results for the linear acoustic absorption coefficient of the large majority of open porosity media. The major inconvenience of this class of models is the non-predictability of the input parameters.

We tried to propose a model adapted to our material in addition to the models previously presented. Indeed, using simply symmetry considerations, we could obtain very easily an elementary cell which did not exchange fluid with its neighbors. By successive slices in this elementary cell we could observe that in the interior of the cell we could consider 6 independent tubes (see figure).

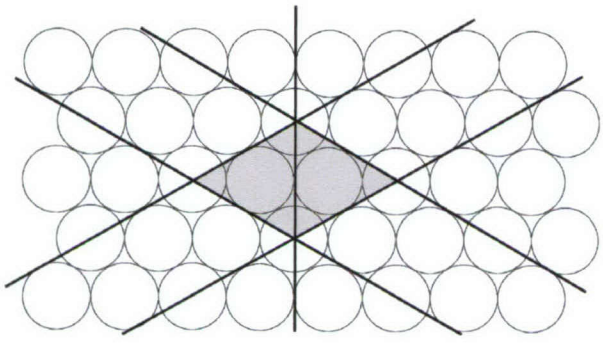

Figure 2 - Elementary cell description

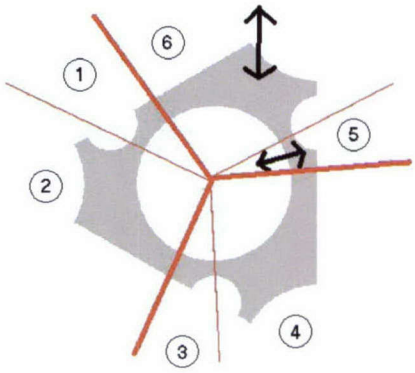

Figure 3 - 6 tubes model

We could now estimate all the necessary parameters for the Biot –Allard [2] model. A good agreement with acoustic absorption experiments was obtained (figure 4).

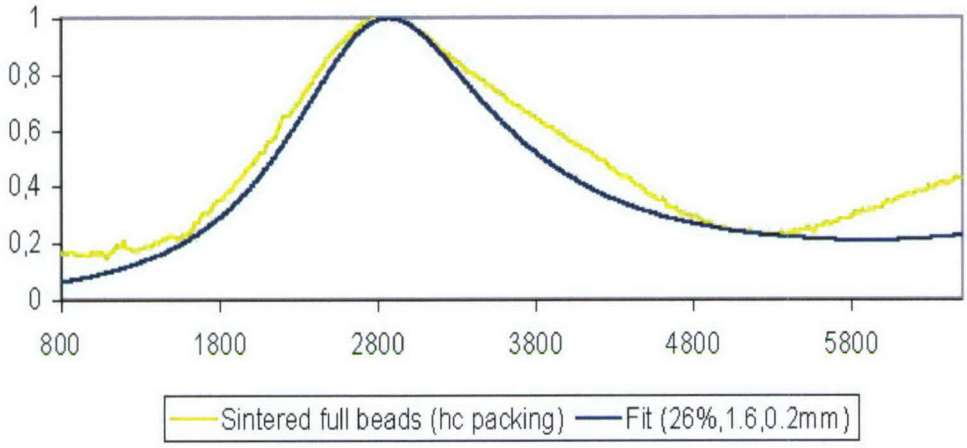

Figure 4 - Measured acoustic absorption coefficient and best fit for a HC packed specimen of full beads with 3.2 mm diameter, 26% porosity, 1.6 acoustic tortuosity and 0.2 effective dynamic radius

4.1.3. Predictive 3D Finite Elements Code Approach – Software development

To have more accuracy we have developed a numerical method based on a homogenization theory. We have dealt with the complete Navier Stokes equations written in a Fourrier assumption with complex number coefficients. For a more detailed treatment the reader is refered to the scientific annexes.

An important effort has been made in order to develop this new 3D code to predict the acoustic wave propagation inside a porous material. This kind of 3D code had never before been developed (at least, according to the literature). A detailed presentation of the numerical approach can be found in [4-6].

One of the most difficult problems was to obtain the necessary adapted mesh (very refined on the border layer close to the solid metallic surface of the inner space between the hollow spheres) in order to reach the high frequencies – up to 10 kHz. The acoustic boundary layer appearing at high frequencies becomes so small ($1/(\omega)^{1/2}$ –dependence, with ω - angular speed) that it imposes meshes with more then 2000000 points to obtain accurate results (more then 5 points inside the layer). This is very prohibitive in computing time costs.

Our difficulties to develop adaptive meshing methods brought us to meet Professor Paul-Louis George at INRIA (Research laboratory in informatics and applied mathematics) who is one of the best specialists in meshing methods in the world. He kindly accepted a scientific discussion with us on this subject and gave us sufficient arguments to abandon this development (he is leading an important team of specialists working on this subject and he confirmed us that there are no other solutions developed elsewhere). He proposed us a simplified solution to our problem. He gave guidelines to the construction by Simulog (industrial partner of INRIA) of an anisotropic adapted mesh to our problem (interstitial volume of a FCC packing of spheres periodic elementary cell). Actually, this represents the best solution to our problem.

FEVRIER 2005

The obtained mesh (figure 5) is perfectly adapted to our problem at any frequency less than the frequency for which the mesh was designed - 50 kHz. It was constructed after we had estimated the thickness of our acoustic boundary layer for a particular frequency (30 microns at 50 kHz for the thermal acoustic boundary layer).

Figure 5 – Adapted mesh for 50 kHz

Figure 6 – Acoustic imaginary temperature field at 50 kHz

The use of this mesh gave us good results for the thermal solution of the acoustic propagation problem (figure 6-7) and calculations for the dynamic solution of the acoustic propagation problem provided good results also (figure 8).

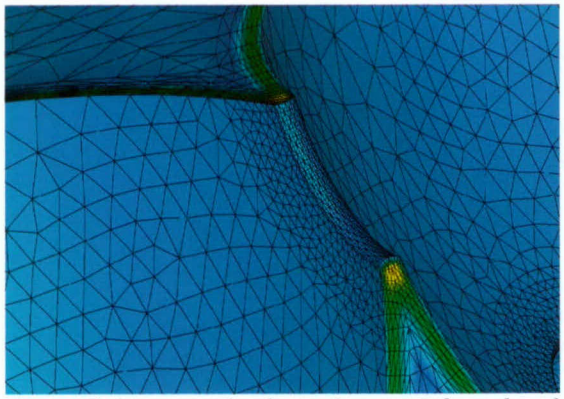

Figure 7- Zoom on the thermal acoustic boundary layer for figure 5 presented field

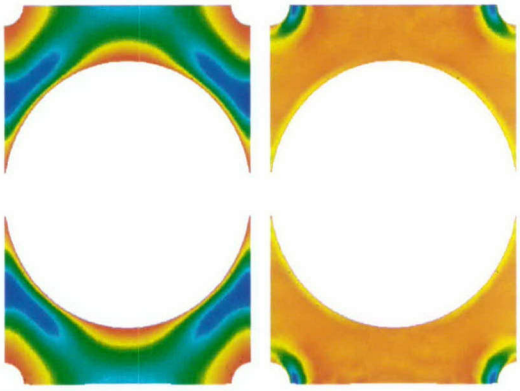

Figure 8 - Example of computed acoustic speed field at 0 respectively and 10 kHz shown in tetragonal section of a FCC network

Figure 9 presents a comparison between our calculated points and the best fits obtained with the acousticians existing models [2]. The good agreement of these curves confirms the predictability of our 3D code.

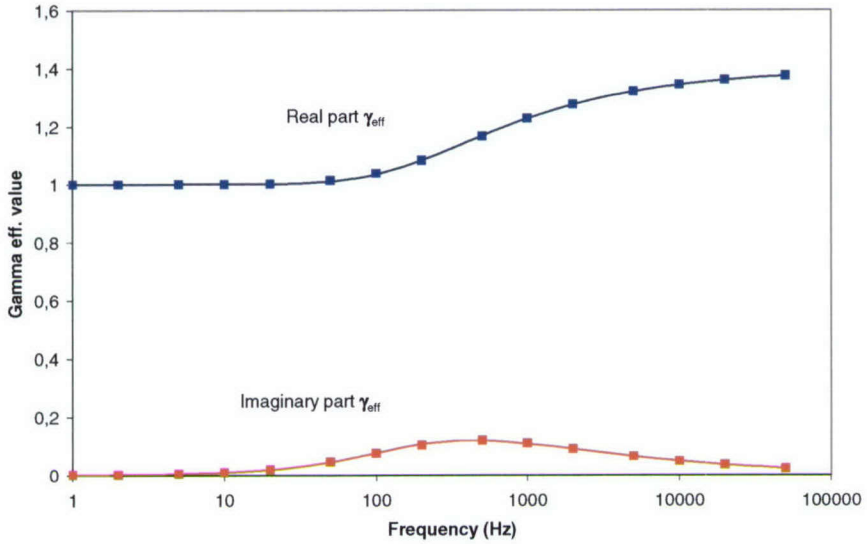

Figure 9 – Comparison between acousticians fits with $\Lambda = 2.39*10^{-4}$ m, C = 1.4, P = 0.49 as parameters [5] and our computed points for γ_{eff}

We could thus provide parameters for the phenomenological approach without measurements or we could describe the behavior on a complete range of frequencies for any porous material with a meshable internal geometry.

4.1.4. Acoustic behavior of a cellular material under a thermal gradient

We have develop a new type of testing machine which measures the acoustic absorption for test specimens loaded with various thermal gradients. We have also proceeded with our first experiments [8].

The developed apparatus is shown in the following figures :

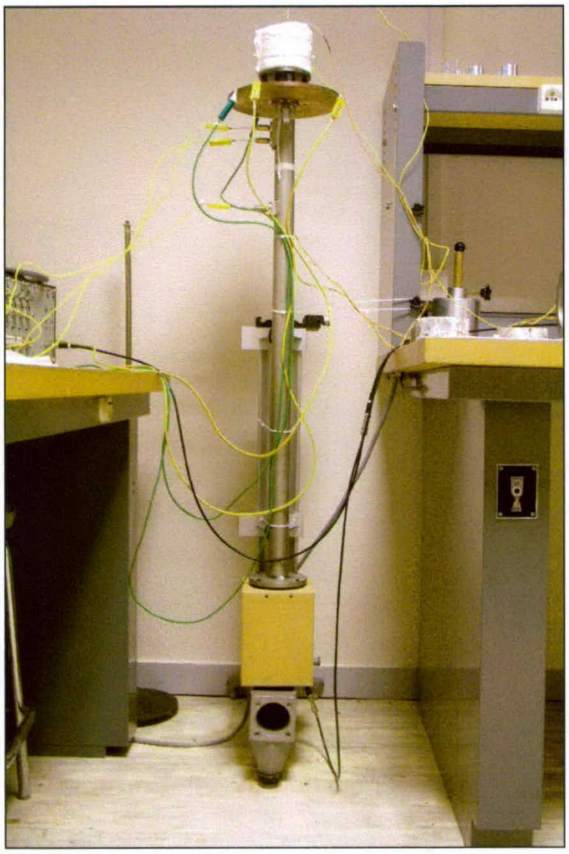

Figure 10 – Modified Kundt tube for acoustic absorption measurements under thermal gradient

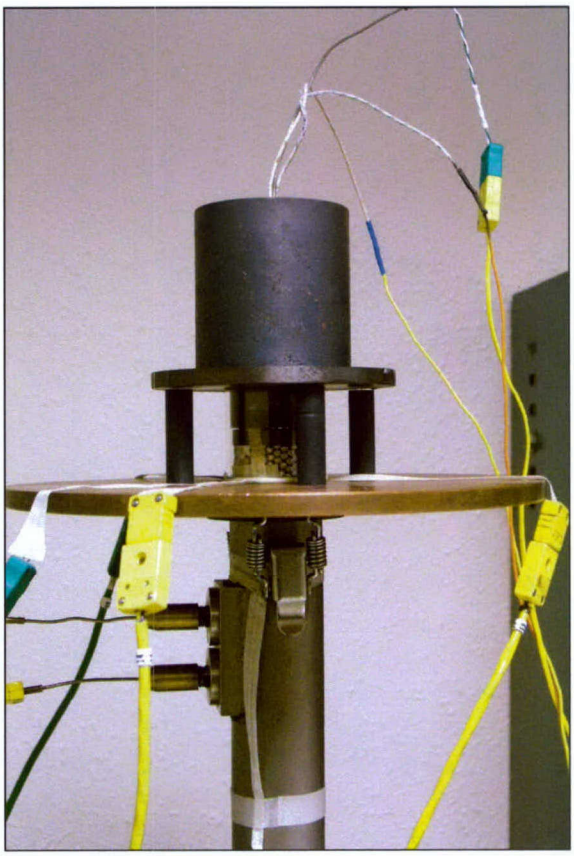

Figure 11 - Zoom on the heating system and the thermal gradient loaded test specimen isolated by a quartz tube

The test specimen was instrumented with 3 thermocouples - as shown in the figure 11 - and the different measurements are reported in table 1.

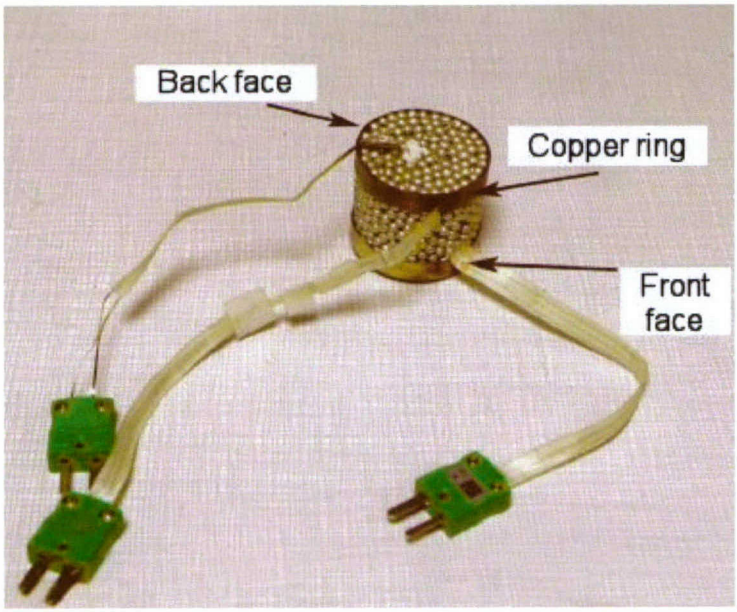

Figure 12 – Instrumented test specimen

Centre of the heated facet (°C)	Border of the heated facet (°C)	Centre of the cooled facet (°C)	Border of the cooled facet (°C)	Axial thermal gradient (K/m)	Radial thermal gradient (K/m)
18	18	18	18	0	0
50	50	36	31	400	360
100	101	67	50	940	1200
150	150	98	69	1500	2100
198	197	124	89	2100	2500
247	248	153	112	2700	2900
290	287	174	131	3300	3100

Table 1 – Registered temperatures and their corresponding installed thermal gradient

The acoustic absorption experiments gave the following absorption curves:

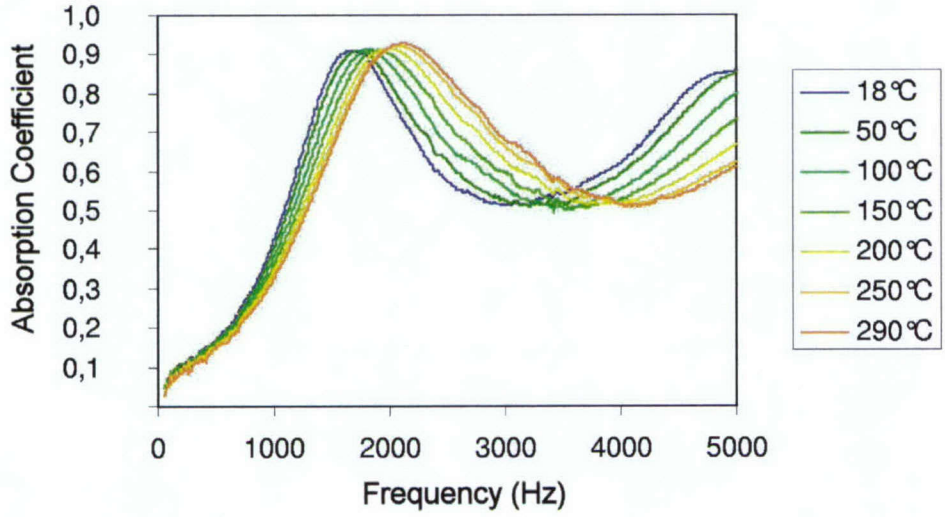

Figure 13 – Absorption curves obtained for different thermal gradients

We have developed a multilayer acoustic absorption model [9]. We have verified this model by comparing our calculus to the acoustic absorption obtained curves. Figure 14 shows this good agreement between the model and experience.

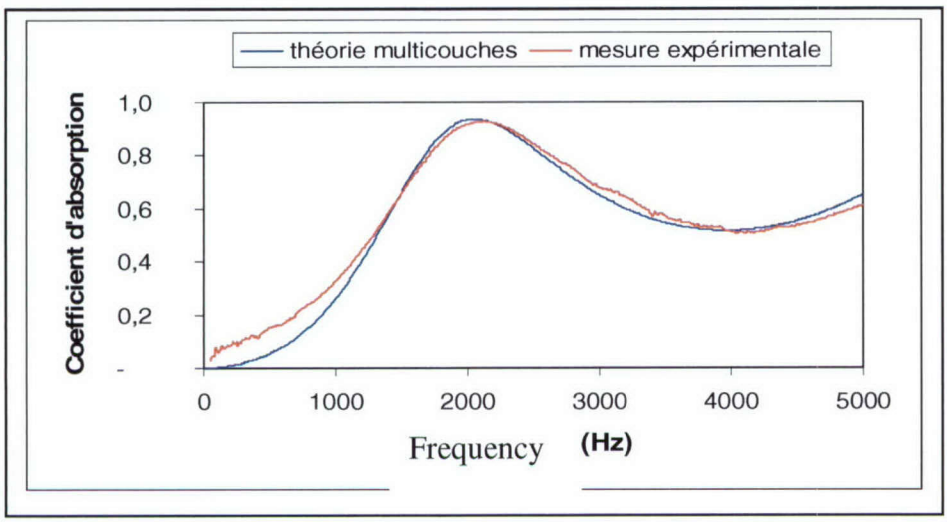

Figure 14 – Comparison between multilayer model (blue line) and registered acoustic absorption(red line) curve for the test specimen loaded with 3300 K/m thermal gradient

To summarize our acoustics study, we have developed and validated a new 3D acoustic absorption FEM code for sound propagation inside porous media [5]. We have also developed a method to test the acoustic behavior under thermal gradients on this type of material and the associated model required to calculate it.

4.2. Mechanics

4.2.1. Elasticity

Our first modeling results stated that a law in two powers of the relative density could fit very well with the Young Modulus of our material. An Ashby [10] type law, calculating analytically the Young Modulus for different hollow sphere diameters and brazing meniscus diameters, was proposed.

$$\frac{E^*}{E} = 0.7 \times \left(\Phi^2 \left(\frac{\rho^*}{\rho} \right)^2 + (1-\Phi) \left(\frac{\rho^*}{\rho} \right) \right) \quad \text{where} \quad \Phi = \frac{1}{2} \times \left(\frac{dm}{db} \right)^{-\frac{1}{4}}$$

and ***dm***, ***db***, are respectively welded joint and bead diameters. We also presented the perfect correlation between this law and our numerically obtained results for an entire spectrum of parameters. But this law has no physical agreement.

Actually, in Ashby's assumption, the meniscus could be accepted as representing the "links between cells". The Φ will be the weight parameter of these links. Or, it could be easily observed that if *dm* increases, Φ will decreases. This is in complete contradiction with Ashby's theory.

We have analysed this contradiction and we have deduced that the problem comes from the physics used by the Ashby theory (bars and membranes) which are different from the physics given by the topology of our material. Indeed, if we start the understanding of the mechanical behavior of our material by the analysis of the shells behavior we could easily deduce a new law respecting the physics.

$$\frac{E^*}{E} = \left(1.5\frac{dm}{db} + 0.287\right)\left(\frac{\rho^*}{\rho}\right)^2 + \left(1.0\left(\frac{dm}{db}\right)^2 + 0.5\frac{dm}{db} + 0.04\right)\left(\frac{\rho^*}{\rho}\right)$$

More details about this new theory could be found in [11].

In order to obtain more accurate results we prefer to choose other parameters for the elastic properties predictions of our cellular material. These parameters were chosen corresponding to the internal geometry of our material and directly related to the processing parameters. We have performed computer simulations on 25 types of FCC hollow spheres based materials. The hollow sphere diameter was fixed at 3 mm and the investigated range for the meniscus radius - r - was between 50 to 300 microns. The thickness of the hollow sphere - t - was analyzed between 20 to 100 microns.

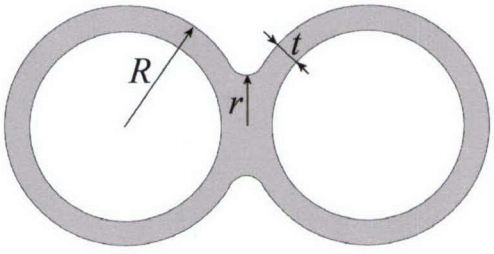

Figure 15 : Characteristics of the welding neck

The numerical simulations were performed on a representative elementary cell and the results provided the macroscopic elastic properties of the material. We have used the homogenization theory and the boundary conditions were imposed repecting this theory.

The table 2 presents these results :

r (µm)	t (µm)	E^* (MPa)	ν^*	G^* (MPa)
100	20	503	–0,492	391
	40	1090	–0,443	775
	60	1790	–0,382	1141
	80	2600	–0,305	1493
	100	3450	–0,242	1820
150	20	598	–0,453	434
	40	1370	–0,383	883
	60	2210	–0,331	1320
	80	3170	–0,271	1740
	100	4190	–0,220	2140
200	20	752	–0,374	482
	40	1700	–0,301	980
	60	2700	–0,266	1470
	80	3850	–0,210	1960
	100	5070	–0,164	2430
250	20	939	–0,285	531
	40	2090	–0,213	1070
	60	3240	–0,189	1610
	80	4600	–0,134	2150
	100	6020	–0,101	2680
300	20	1140	–0,204	583
	40	2500	–0,128	1170
	60	3850	–0,103	1750
	80	5410	–0,0606	2330
	100	7030	–0,0372	2860

Table 2 : Numerical results for the elastic properties of the porous material; the elastic properties of the constitutive material that was used here are $E = 190$ GPa and $\nu = 0.4$.

We deduced 3 analytical non dimensional laws for the elastic properties E^*, G^*, ν^* estimated for the [1 0 0] FCC direction :

$$\frac{E^*}{E} = \left(5.14\left(\frac{r}{R}\right)^2 + 0.587\frac{r}{R} + 0.118\right)\frac{t}{R} + \left(-30.1\left(\frac{r}{R}\right)^2 + 10.5\left(\frac{r}{R}\right) + 0.826\right)\left(\frac{t}{R}\right)^2$$

$$\frac{G^*}{G} = \left(-3.29\left(\frac{r}{R}\right)^2 + 2.59\frac{r}{R} + 0.253\right)\frac{t}{R}$$

$$\nu^* = \left(-13.6\frac{r}{R} + 5.7\right)\frac{t}{R} + 2.58\frac{r}{R} - 0.75$$

where E and G are the elastic moduli of the constitutive material.

In a recent paper, Sanders and Gibson [12] have calculated the elastic properties of a similar regular stacking of hollow spheres, in a range of parameters (t/R; r/R) which was different from the one we have investigated here.

We have compared our results to the ones obtained by Sanders & Gibson at MIT.

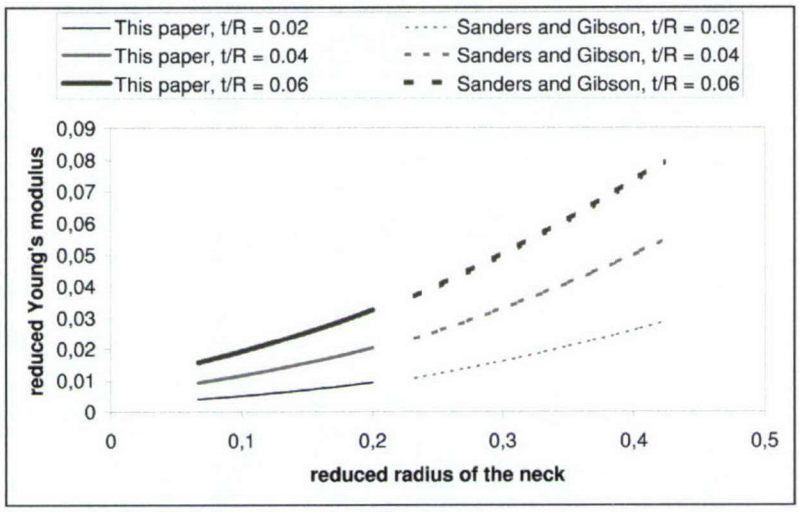

Figure 15: Comparison of this work results with the results of Sanders and Gibson : the reduced Young's modulus E^*/E is plotted as a function of the reduced radius r/R of the welding neck for three different reduced thicknesses t/R.

Although both numerical results seem to extrapolate each other, the expression proposed by Sanders and Gibson [12] fails to describe accurately situations where the normalised meniscus diameters between the hollow spheres are very small. We have also carried compression experiments. The measured Young Moduli were not in agreement with those that were calculated as presented in table 3.

R (mm)	t (µm)	t/R	E^* experimental (MPa)	E^* calculated for $r = 0$ (MPa)
3	150	0,05	430	1200
3	120	0,04	350	930
3	90	0,03	340	650
2	150	0,075	1700	2100
2	120	0,06	860	1600
2	90	0,045	370	1100
1	150	0,15	2100	6000
1	120	0,12	2100	4200
1	90	0,09	830	2700

Table 3 – Comparison between calculated and measured Young Modulus

This non agreement could be explained by a processing default. We have used improved Ni hollow spheres. They had no more walls holes but they have shown (after microscopic analysis) a significant scatter in their wall thickness.

Another problem came from the brazing method. We discovered that the concentration in P of the NiP brazing chemical deposit was not the indended value - despite that the test specimens seem to be "correct" - see figure 16. As shown in figure 17 the temperature level that we have used for the brazing processing was not enough to assure a completely melting of the NiP deposit.

We present in the figure 18 the typical observed meniscus which definitely could not be represented by our FEM calculation.

We are currently working to improve the entire brazing system and we will likely use a NiB diffusion system for the assembling of our material.

We maintain that our predictive laws are complementary to the MIT-deduced laws. The experimental results have shown that our predictions respect the order of magnitude of the measured Young Modulus.

No other existing experimental validations were found in the literature except for the works of T.J. Lim [13]. They have obtained results qualitatively similar to ours but for non-regularly packed Hollow Spheres structures. Unfortunately they have measured only one ratio between the meniscus and the sphere diameter material and they have not investigated the influence of the meniscus diameter on the elastic properties. Further work is necessary in processing improvements to validate the set of complementary predictive laws proposed by ONERA and MIT for the Hollow Spheres based FCC packed cellular materials.

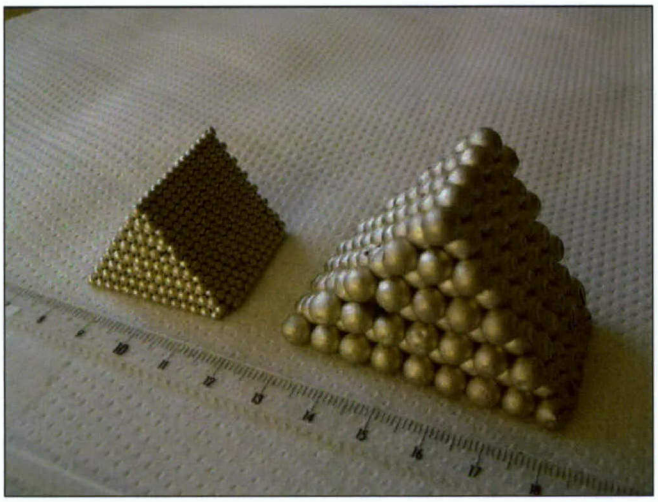

Figure 16 – FCC test specimens with 2 mm and 6 mm hollow spheres diameters

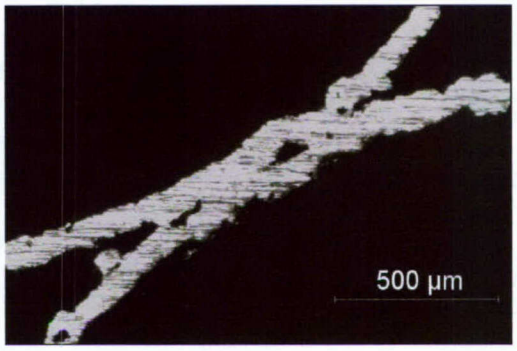

Figure 18 – Typical « wrong » meniscus

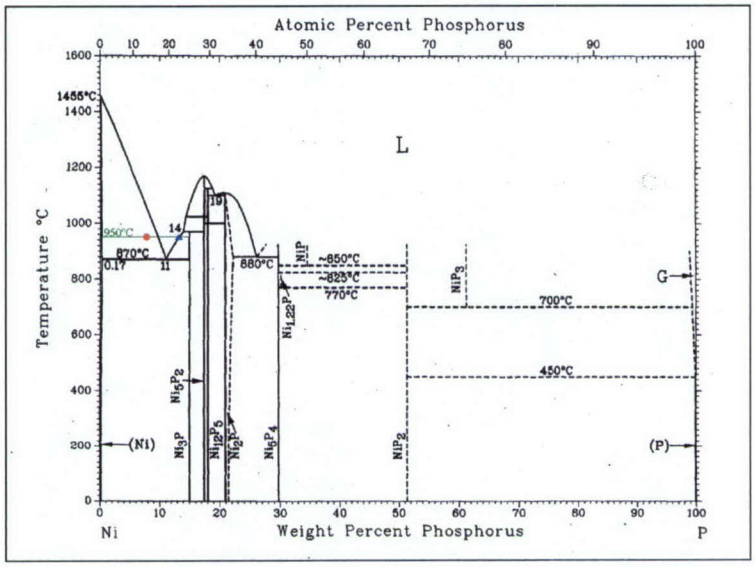

Figure 17 – NiP diagram explaining that for the red plotted point we have no completely melted the brazing deposit

More details concerning our elasticity results and deduced laws are presented in the published papers in Scripta Materialia [11] and Material Science and Engineering [14].

4.2.2. Macroscopic yielding criterion for HS based cellular material

Once the elasticity was perfectly described, our attention was focused on the macroscopic elastic limit. The obvious difficulty for this type of material was determining how to reveal the local microscopic plastic deformation under a macroscopic loading. As we have chosen to study a regular material, FCC packing of hollow spheres, which are bonded together by a joining technique (sintering, brazing, or soldering), they are presented again in figure 19.

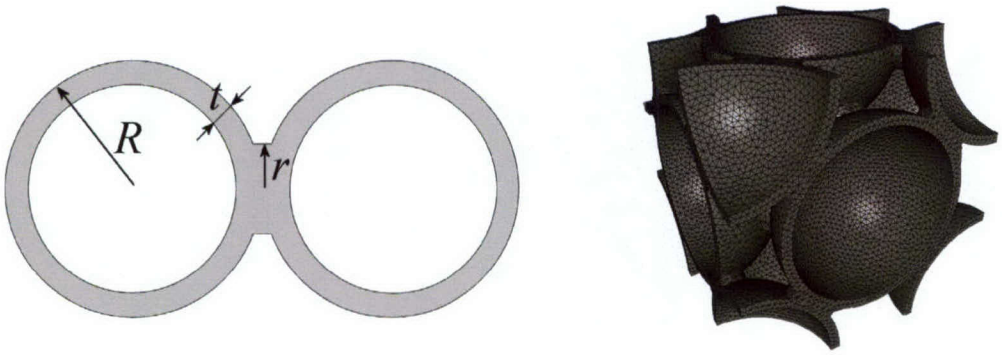

Fig 19: a) Geometric description of the PHS structure b) Mesh of the PHS elementary cell

The microplasticity of this material, *i.e.* the criterion indicating when the condition for the plasticity of the constitutive material is reached locally, was the focus of our work. Since microplasticity is concerned with the onset of plasticity, its conditions can be derived from the consideration of linear elasticity only, coupled with plastic threshold conditions.

The present report briefly introduces the method we developed to compute the yield surface of a periodic cellular material from the yield criterion of the constitutive material.

4.2.3. Computation method

The approach is based on linear elasticity and on homogenisation. It is well known [15,16] that a heterogeneous elastic material with a periodic structure can be described at a macroscopic scale much larger than the size of the elementary cell of the lattice as an equivalent homogeneous elastic solid. By the virtue of the superposition principle for linear elasticity, the elastic tensor can be completely computed as soon as the stress and strain fields have been computed for 6 independent loading cases which are compatible with the periodic boundary conditions. Each loading case corresponds to a *macroscopic strain tensor,* $\underline{\underline{E}}$, which defines the boundary conditions to apply on the representative cell and to a *macroscopic stress tensor,* $\underline{\underline{\Sigma}}$, which can be computed by averaging the stress field over the complete representative cell with the assumption of null stress in the pores (a detailed description can be found in [15]). In this way, one obtains 6 independent relationships between macroscopic stresses and the macroscopic strains; as the stress and strain tensors are a symmetric second order tensor, they belong to a 6-dimensional space, and the 6 linear relations therefore define completely the fourth order elastic tensor that links them.

Each *macroscopic tensor,* $\underline{\underline{\Sigma}}$, applied on the representative cell will produce inside the material a local stress tensor $\underline{\underline{\sigma}}(\underline{x}) = \underline{\underline{\underline{\underline{M}}}}(\underline{x}) : \underline{\underline{\Sigma}}$ (1)

Here, $\underline{\underline{\Sigma}}$ represents the macroscopic stress field, $\underline{\underline{\sigma}}(\underline{x})$ is the local stress tensor at point $\underline{x}$, and $\underline{\underline{\underline{\underline{M}}}}(\underline{x})$ is a fourth order tensorial field, called the *scale tensor*.

This condition holds whenever the material behaves everywhere elastically. If the constitutive material has an elastoplastic behavior, equation (1) holds as long as the yield criterion is not reached at any point $\underline{x}$ of the structure. This can be rewritten as:

$$\max_{\underline{x}} f\left(\underline{\underline{\sigma}}(\underline{x})\right) < 0 \qquad (2)$$

Now, the linear relationship (1) can be injected in (2), yielding the condition on the macroscopic loading $\underline{\underline{\Sigma}}$ translating that the onset to microplasticity has not been reached:

$$\max_{\underline{x}} f\left(\underline{\underline{\underline{\underline{M}}}}(\underline{x}) : \underline{\underline{\Sigma}}\right) < 0 \tag{3}$$

Since $\underline{\underline{\underline{\underline{M}}}}(\underline{x})$ is an intrinsic quantity of the porous material, (3) can be seen as a "non yield" criterion for the porous structure:

$$F(\underline{\underline{\Sigma}}) < 0, \quad F(\underline{\underline{\Sigma}}) \equiv \max_{\underline{x}} f\left(\underline{\underline{\underline{\underline{M}}}}(\underline{x}) : \underline{\underline{\Sigma}}\right) \tag{4}$$

Here, F provides a macroscopic yield criterion for microplasticity: when F reaches zero for a given load $\underline{\underline{\Sigma}}$, there exists a position in the structure where the stress reaches the yield criterion of the constitutive material. This criterion, by construction, can also handle multiaxial loadings, so (4) can describe the anisotropic character of the porous structure yielding, even if the constitutive material is plastically isotropic. Such an anisotropic yield criterion is needed if one intends to model the porous material as a homogeneous material in an intricate system where it will possibly experience complex loadings.

Equation (4) can hardly, if ever, be handled analytically in a porous structure. Therefore, a numerical approach must be used instead. In particular, the use of FEM is suitable, as the maximization over a continuous domain in (4) can be straightforwardly replaced by maximization over a discrete set of integration points. Let $\underline{\underline{\Sigma}}_1, \ldots \underline{\underline{\Sigma}}_6$ be six linearly independent loadings, and let $\underline{\underline{\sigma}}_1(\underline{x}), \ldots \underline{\underline{\sigma}}_6(\underline{x})$ be the six corresponding stress fields.

For any macroscopic stress tensor $\underline{\underline{\Sigma}}$, which corresponds to a given macroscopic loading, one can consider its proportional loadings $\lambda\underline{\underline{\Sigma}}$. As the condition $f(\underline{\underline{\Sigma}}) < 0$ defines a convex domain in the 6-dimensional stress space, there exists a positive coefficient λ depending on $\underline{\underline{\Sigma}}$ such that $f(\lambda\underline{\underline{\Sigma}}) = 0$, and $f(\mu\underline{\underline{\Sigma}}) < 0$ for any positive $\mu < \lambda$, that we shall denote by $\lambda(\underline{\underline{\Sigma}})$. By convexity of the elastic region, the set of all the stress tensors of the form $\lambda(\underline{\underline{\Sigma}})\underline{\underline{\Sigma}}$ (where $\underline{\underline{\Sigma}} \neq \underline{\underline{0}}$ is arbitrarily obtained by randomizing on the six linearly independent loading cases) defines the yield surface. Thus, to obtain this yield surface, it is sufficient to compute $\lambda(\underline{\underline{\Sigma}})$ for any macroscopic loading $\underline{\underline{\Sigma}}$, or more pragmatically to compute it for a large enough random set of macroscopic loadings.

4.2.4. Computed results

In the following, we will consider (4) for the case of an isotropic constitutive material, the yield criterion being chosen as the von Mises criterion:

$$f(\underline{\underline{\sigma}}) = \sqrt{\frac{3}{2}\left(\underline{\underline{\sigma}} - \frac{1}{3}\mathrm{tr}\,\underline{\underline{\sigma}}\right) : \left(\underline{\underline{\sigma}} - \frac{1}{3}\mathrm{tr}\,\underline{\underline{\sigma}}\right)} - \sigma_y \equiv g(\underline{\underline{\sigma}}) - \sigma_y \tag{5}$$

where σ_y is the yield stress of the constitutive material in the case of uniaxial loading. This choice implies in particular that $F(\underline{\underline{\Sigma}})$ is invariant when $\underline{\underline{\Sigma}}$ is replaced by $-\underline{\underline{\Sigma}}$.

The geometry of the porous medium, which will govern the scale tensor, is characterized by the hollow sphere radius R and thickness t, and by the shape and size of the necks bonding the spheres together (as presented in figure 19).

For the sake of simplicity, the bonding necks are modelled as straight cylinders of radius r (see fig. 19a). The chosen values of t/R and r/R for this reported computation were respectively 0.1 and 0.3.

In a plastically isotropic material the yield surface can be drawn as a curve in the plane consisting of the Von Mises equivalent stress and the hydrostatic stress. The yield surface for our cellular material is displayed on fig. 20 in this set of coordinates. Using randomly selected stress tensors $\underline{\underline{\Sigma}}$, we computed the corresponding $\lambda(\underline{\underline{\Sigma}})$ and project $\lambda(\underline{\underline{\Sigma}})\underline{\underline{\Sigma}}$ in that plane. The result is a yield "cloud" allowing one to visualize the projection into a plane of the 6-dimensional space yield surface. The scatter of the representative points reflects plastic anisotropy.

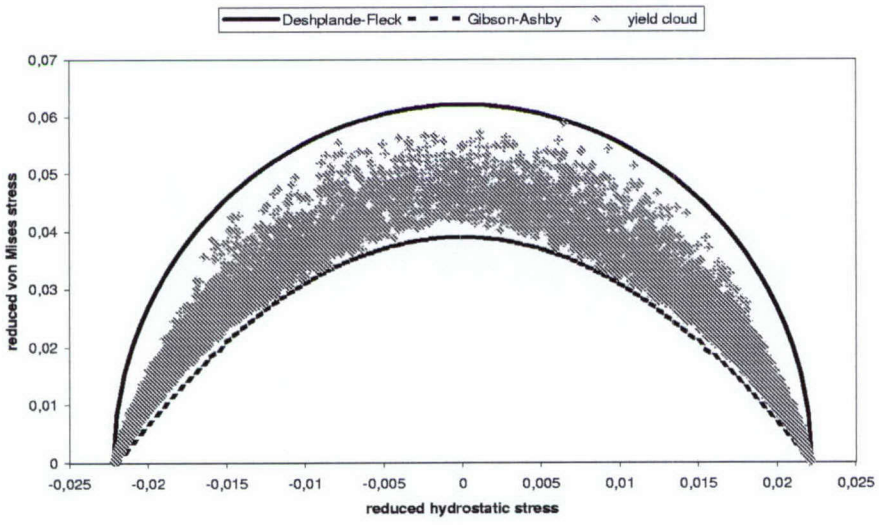

Fig. 20: Projection of the yield surface on the hydrostatic macroscopic stress vs. von Mises macroscopic stress plane; the stresses are divided by the yield stress σ_y of the constitutive material to get dimensionless quantities referred to as reduced stresses.

Despite the anisotropy of the structure, which forbids describing the yield criterion as a function of the stress invariants only, it is still worth comparing the results of the FEM calculation to the isotropic yield criteria which have been proposed for metal foams. Fig. 20 displays two lines bounding the yield cloud; the lower bound is a parabola and the upper bound is an ellipse. These two shapes correspond to the Gibson-Ashby [10] and Deshpande-Fleck [17] criteria respectively:

$$F_{GA}\left(\underline{\underline{\Sigma}}\right) = \Sigma_{eq} + C_1 \frac{\Sigma_h^2}{\Sigma_1} - \Sigma_1 \tag{6}$$

$$F_{DF}\left(\underline{\underline{\Sigma}}\right) = \frac{\Sigma_{eq}^2}{\Sigma_2} + C_2 \frac{\Sigma_h^2}{\Sigma_2} - \Sigma_2 \tag{7}$$

where Σ_1 and Σ_2 are macroscopic uniaxial yield stresses, C_1 and C_2 are positive dimensionless constants, and Σ_h and Σ_{eq} are the hydrostatic stress and the von Mises stress corresponding to the

macroscopic stresses. Here, the values of the constants are respectively $\Sigma_1 = 0.04\sigma_y$, $\Sigma_2 = 0.065\sigma_y$, $C_1 = 3.3$ and $C_2 = 8.7$.

4.2.5. Discussion and conclusions on the macroscopic established yield criterion

We developed a new method to calculate the anisotropic 6-dimensional yielding surface for porous materials which complete perfectly the existing criteria of Gibson & Ashby [10] or Deshpande & Fleck [17]. These results, applied to a hollow spheres structure, were published in the Scripta Materialia Journal [18].

A complementary study, analytically relating the yield criterion to geometrical parameters, is a natural extension of this work. A simple analytical tool will thus be available for complete engineering design. As the Deshpande-Fleck provides an upper bound of the yield cloud, it corresponds to a criterion ensuring that microplasticity occurs in the material. On the contrary, the Gibson-Ashby criterion, which provides a lower bound, can be used as a conservative dimensioning criterion when plasticity is to be avoided.

Beyond its application to the PHS geometry, we want to highlight the efficiency of the proposed method to deal with microplasticity of periodically structured porous media. It should be noted that any other local yield criterion $\phi(\underline{\underline{\sigma}})$ would be suitable to this approach, but if $f(\underline{\underline{\sigma}}) = g(\underline{\underline{\sigma}})$-$\sigma_y$, where g is an homogeneous function of first degree (for instance the Tresca criterion), the computation of $\lambda(\underline{\underline{\Sigma}})$ can be obtained in an efficient way.

4.2.6. Creep behavior of the Hollow Sphere based material

The creep behavior of cellular materials was described by Ashby et al. for the classic metallic foams. Andrew & Gibson have developed a 2D model and they also complete some experimental tests on open Al and Ni foams. We haven't found any other creep characterization for Hollow Spheres structures in the literature.

Some test specimens of our hollow spheres based material were tested. The test specimens were processed with 2.5 mm diameter spheres, 80 µ averaged wall thickness and brazed with 4 µ NiB deposit. We proceeded to creep tests on 10x10x10 mm cube test specimens at 600 °C. A standard typically registered curve is presented in the next figure (21). He have used 3 different loadings corresponding to 0.2 , 0.6 and 1.8 MPa macroscopic load.

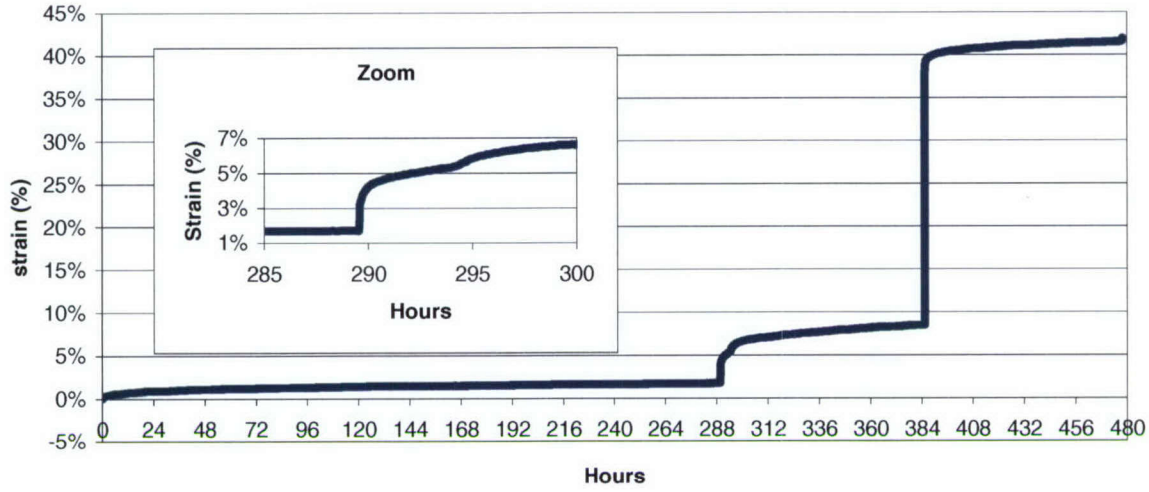

Figure 21 - Standard registered creep curve

We can highlight several important observations:

- The material could support loadings at a very high level of macroscopic deformation. Macroscopic strains superior to 40% were efficiently accommodated by the material. By local buckling of the spheres, the material reacts on the loading and it adapts its strength. New first stage creep behavior occurred at any loading level followed by a very clear second stage each time.

- In the period corresponding to the second loading level of this typical creep experiment a strange inflexion occurred in the registered results (we have obtained this inflexion for other experiments also). The zoom presented in the figure shows that something real was happening. Two explanations seem possible to us: sphere walls oxidation and/or creep-buckling of the hollow sphere's shell type structure.

The wall oxidation will induce a slow modification of the structural properties and this could not be captured on the registered creep curve, unless the oxidized part of the wall delaminates. Thus, the stress will be redistributed and a new first stage creep will initiate.

The "creep-buckling" mechanisms could occur by the slow modification of the local geometry of the internal structure, which experiences stress re-distribution at the particular moment when a sphere wall locally buckles. This also could initiate a new first stage creep mechanism for the entire structure of the cellular material.

To summarize, our creep experiments, carried for the first time on Hollow Sphere-based cellular materials, showed a very complex creep behavior. We have probably identified two specific creep mechanisms for these structures in addition to the classic mechanisms. We suggest for further investigations in-situ 3D tomography experiments as the only type of experiments able to accurately confirm our suppositions or clearly established the creep mechanisms of these cellular materials.

4.3. Optimized Design

4.3.1. Introduction

Materials and process selection methods in mechanical design has evolved drastically in the last ten years, leading to the development of integrated software, using hierarchical databases and graphical analysis, allowing one to deal with multicriteria selection (for recent review, see [19-23]).

Another strategy for optimal design is to develop "taylored materials", i.e. materials which are specifically designed for a precise set of requirements. Such an approach, developed for composite materials as an example, or sandwich structures with a foamed core [24,25], requires on one hand databases for constituent materials, and on the other micromechanical models allowing the prediction the properties of the "tailored material" as function of its individual constituents.

The material is composed of constituents, but is considered as a new material which can be described as such and evaluated using the classic selection procedure. Selection software relying on the use of genetic algorithms as optimization tools have been developed as examples of this new type of design strategy [26].

The design of hybrid materials and the development of "tailored solutions" become more and more important with the emergence of multifunctionnal materials: very often, complex multifunctionnality cannot be dealt with using a single bulk material. Multimaterials with explicit optimization of the geometry which dictates the organization of the constituents are often the most efficient solution. We proposed to investigate the best optimized solutions using our HS-based cellular material for acoustic liners in the high temperature exhauster of an aircraft engine.

4.3.2. Qualitative analysis of the requirements for noise reduction

We will first recall some important requirements and the normally selected choices. The operating temperature (more than 800°C for civil and 1000°C for military engines) obviously rules out polymeric materials, and the requirements of damage tolerance if the acoustic absorbant is expected to have some structural properties, rules out the ceramic material. The constitutive materials have to be from the class of metallic alloys (or possibly metal matrix composites). The efficiency of the acoustic component requires that a substantial part of an incoming pressure wave penetrates the material and is progressively dampened via dissipation processes in the material. This requires that the acoustic impedance (roughly speaking, the density times the sound velocity) mismatch between the material and the gas is minimal. The selection of bulk metallic alloys would thus be extremely poor for the acoustic mismatch, and in addition, the damping coefficient never exceeds 2%. As a consequence, one is naturally led to consider solutions in which the gas carrying the pressure wave penetrates the material: the acoustic dissipation resulting from shear viscous flow of the gas inside the spaces in the material. One is naturally led to porous materials. We want thus to develop a material which has some structural integrity, and in addition, which can be controlled in a way that optimum absorption for a given noise spectrum can be obtained.

FEVRIER 2005

The proposed solution will investigate a structure containing our developed material consisting of a regular array of hollow metallic spheres bonded together, stacked in a FCC arrangement. Such a principle presents the open porosity necessary for sound absorption, the closed cellular structure responsible for good specific stiffness and specific strength. The simplicity of the geometry allows in principle a robust optimization. A picture representing the structure is shown in figure 22a, and the geometrical variables entering the optimization procedure is shown in figure 22b, figure 22c gives a schematic of the material's implementation on a macroscopic scale.

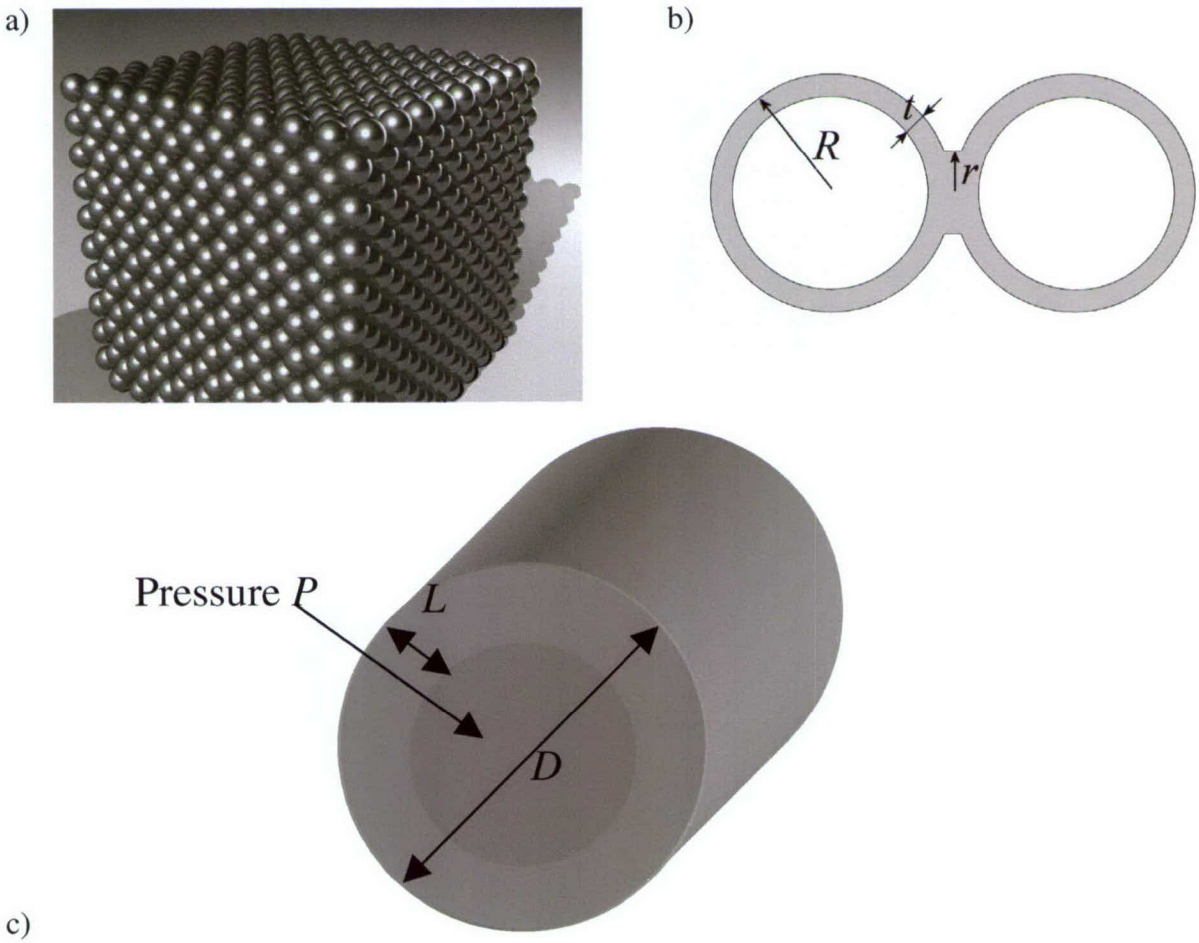

Figure 22: Solution of regular FCC stacking of hollow metallic spheres. a) 3D representation of the material b) local geometry c) geometry of the material implemented in the system: schematics of a cylindrical shell for sound absorption

The parameters accessible for optimization of the material are the following: the radius R of the spheres and their thickness t, the dimensions r of the necks connecting spheres together and of course the properties of the constituent material (m). The acoustic liner will be implemented as a coating surrounding the engine component where the noise is generated or could be absorbed. The thickness L of this coating is also a possible variable for optimization.

FEVRIER 2005

The multifunctionnal requirements under consideration were simplified for the sake of illustration. The constraints of the problem are such that, under the internal pressure, the choice of the porous material properties (namely elastic modulus E and yield stress σ_y) and the layer thickness L ensures that the structure is stiff enough and remains in the elastic loading regime. With the simple geometry sketched in figure 2b, the two constraints for the stiffness and the strength of a cylinder of diameter D and thickness L under a pressure P can be written:

$$\frac{\partial D}{D} = \frac{PD}{2LE^*} < \varepsilon_{\max} \tag{8}$$

$$\sigma = \frac{PD}{2L} < \sigma_{ys}^* \tag{9}$$

The properties E* and σ_{ys}* are the Young modulus and the Yield stress of the cellular material. ε_{max} denotes the maximum admissible elastic deflection imposed by the designer.

The objectives to be aimed for are a minimal mass and a maximum sound absorption. The quantity to be optimized for mimimal linear mass of the cylinder is straight forward:

$$M=\rho^* .LD \tag{10}$$

where ρ* is the density of the cellular material. The acoustic optimization is more difficult to evaluate. If one denotes by I(ω) the power spectrum to be absorbed, and A(ω) the absorption of a sound wave of frequency ω, the quantity to be maximized is the integral absorption coefficient denoted *Abs* and defined by:

$$Abs \equiv \frac{\int_{\text{spectre}} A(\omega) I(\omega) d\omega}{\int_{\text{spectre}} I(\omega) d\omega} \tag{11}$$

In order to proceed with the optimization procedure, we need an evaluation of E*,s_{ys}*.,r* and A(ω) as functions of the constitutive material's properties (E, σ_{ys}, ρ), of the geometrical parameters of the hollow spheres (R, r, t) and of the macroscopic dimension of the layer L. "Materials by design" presupposes the knowledge of a model able to provide these relationships. Such models have been developed and referred to in the previous chapters and only the results will be recalled in the following section. The following sequence will be guiding our optimization process:

- Optimization of R and L for maximizing acoustic absorption for a given noise spectrum
- Optimization of t and r for ensuring the stiffness and strength constraints at minimal mass, for a prescribed constitutive material
- Optimization of the choice of the constitutive material.

4.3.3. Quantitative analysis of acoustic optimization

For a spectrum which would be concentrated around a specific frequency, the choice of the thickness L will allow the absorption peak to coincide with the emission peak. For a case where the noise spectrum is less peaked, the choice of a smaller size for the spheres will allow an increased efficiency.

FEVRIER 2005

For the sake of illustration of the optimization method we have developed, we will deal successively with two extreme cases of band spectra, shown schematically in figure 23: a spectrum formed by a peak at 3kHz, and a spectrum homogenously distributed between 1 and 5kHz. The case of a general spectrum can be treated following the same lines.

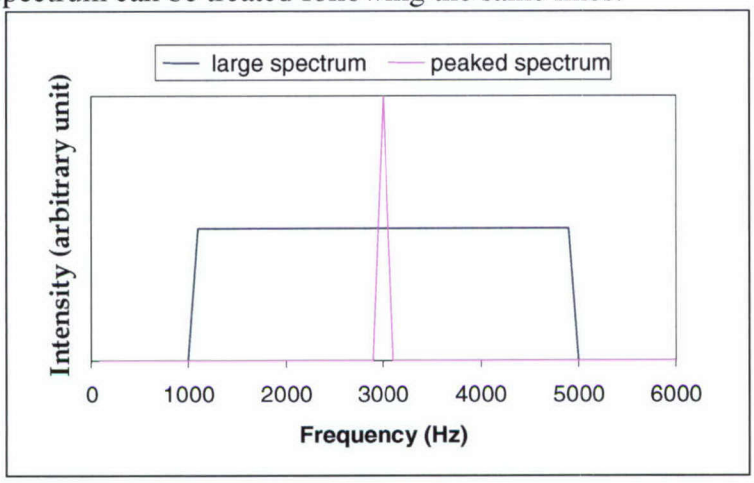

Figure 23 : Schematized spectra used for the illustration of the optimization methodology.

Contours of equal values of the acoustic absorption for the peaked and wide spectra are shown in figure 24a and 24b respectively in a R-L map.

The case of a peaked noise spectra (Figure 24a) shows that the thickness L has to be chosen relatively accurately, and, for a given L there is a range of radii R able to provide the optimum absorption. The optimal values of the thickness correspond to the successive resonances.

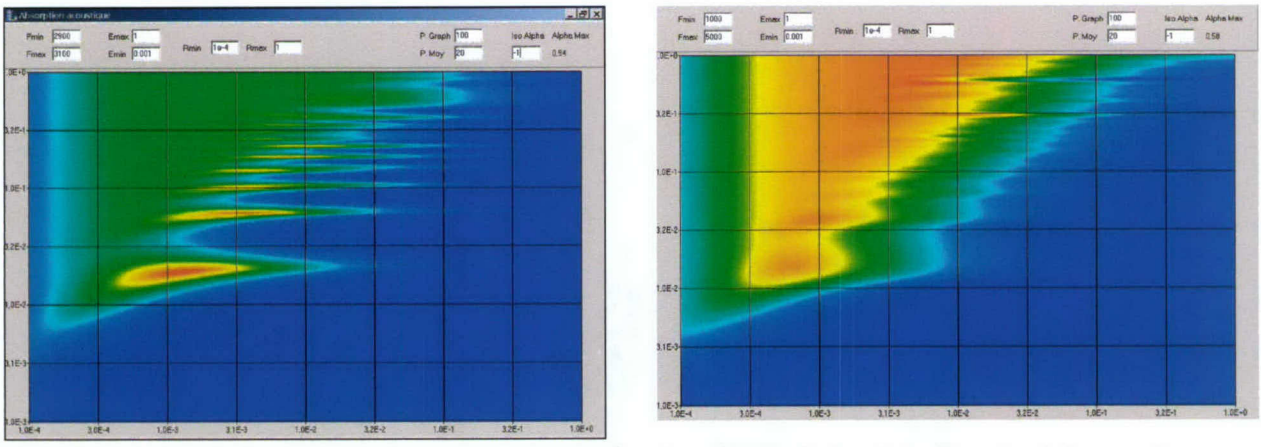

Figure 24: Contours of equal acoustic absorption in the plane R (abscise) – L (ordinate); a) for a noise spectrum peaked at 3kHz, b) for a noise spectrum evenly distributed between 1 and 5 kHz.

The overall picture which emerges from this first step of optimization is that the optimal values of L and R will be driven by the acoustic requirements, whereas the optimization for minimal mass within the mechanical constraint will lead to the choice of the ball thickness t and of the size of the connecting necks r.

4.3.4. Quantitative analysis of Mechanical optimization for minimum mass

Mechanical properties of cellular materials have been extensively studied both experimentally and theoretically. The properties of a regular array of hollow spheres connected by necks have received comparatively very little attention. The standard Gibson Ashby analysis, well suited for open or closed cell structures, is not relevant in the present situation [11]. The dimensionless parameters which will enter the expressions for E*, σ_{ys}*,ρ* as function of E, σ_{ys}, ρ are t/R (which will control the relative density of the cellular solid) and r/R, which reflects the proportion of matter included in the necks. The modelling techniques required to obtain the properties of the cellular solid are Finite Element Calculations [5, 11, 12, 14]. The criterion chosen for plasticity is very stringent since it is identified with the minimum stress for which locally the material yields in a neck or inside a shell.

The value of E*/E as function of r/R and t/R has been obtained via FEM calculations [5, 11].

$$\frac{E^*}{E} = \left(5.14\left(\frac{r}{R}\right)^2 + 0.587\left(\frac{r}{R}\right) + 0.118\right)\left(\frac{t}{R}\right) + \left(-30.1\left(\frac{r}{R}\right)^2 + 10.R5\left(\frac{r}{R}\right) + 0.286\right)\left(\frac{t}{R}\right)^2 \tag{12}$$

The value of σ_{ys}*/σ_{ys} is obtained from a similar type of calculation by Sanders and Gibson [12] rewritten with the same dimensionless variables.

$$\frac{\sigma^*_{ys}}{\sigma_{ys}} = \left(1.10\left(\frac{r}{R}\right) + 0.55\left(\frac{r}{R}\right)^2\right).\left(\frac{t}{R}\right)^{1.13} \tag{13}$$

In a first approximation, we assume that the necks contribute little to the overall mass of the structure. Since both E* and σ_{ys}*are increasing functions of r/R, this suggests the selection of r the maximum value for which the necks touch its neighbor. An approximate expression for this situation is given by :

$$\frac{E^*}{E} = 1.9\left(\frac{t}{R}\right)^{0.92} \quad \text{(calculation by Sanders and Gibson [12])} \tag{14}$$

$$\frac{\sigma^*_{ys}}{\sigma_{ys}} = 3.3\left(\frac{t}{R}\right)^{1.13} \tag{15}$$

The optimization for minimal mass with constraints on rigidity and solidity relies on the optimization of the free variable t/R, and on the choice of the best material. The rigidity constraint (8) together with the expression of E*, imposes a minimum value for (t/r).

$$\left(\frac{DP}{3.8EL\varepsilon_{\max}}\right)^{1.09} < \frac{t}{R} \tag{16}$$

Similarly, the solidity constraint imposes a minimal value too.

$$\left(\frac{DP}{6.6L\sigma_e}\right)^{0.88} < \frac{t}{R} \tag{17}$$

Since the linear mass of the liner is proportionnal to the cellular material's density which in turns is proportionnal to the constitutive material density and to t/R, the quantities to be maximised in the choice of the constitutive material are, for the rigidity and the solidity constraints respectively :

$$M_1 = E^{1.09}/\rho \quad (18)$$

$$M_2 = \sigma_{ys}^{0.88}/\rho \quad (19)$$

The best solutions are limited by strength and can be ordered according to the index M_2. The best 20 materials selected by this procedure in the Cambridge data base [27] are shown in Figure 25.

Material	Index M_2
Alloy Nickel-Cobalt-Chromium, "UDIMET 700"	54
Alloy 79Ni-4Mo-Fe cold rolled	51
Alloy Nickel Cobalt cast	51
Alloy Nickel-Chromium-Cobalt, "MAR-M 421" cast	51
Alloy Nickel-Iron "Alliage 2A", cold rolled	49
Alloy Nickel-Chromium-Cobalt, "IN-738LC", cast	49
Alloy Nickel-Chromium-Cobalt, "NIMONIC 115", thermally treated	49
Forged autenistic stainless steel, AISI 201	48
Forged autenistic stainless steel, AISI 202	48
Alloy Nickel Cobalt	47
Alloy Nickel-chromium-cobalt-molybdenum, Rene 41, STA	47
Forged autenistic stainless steel, AISI 302, traité thermiquement	47
Alloy Nickel-Cobalt-Chromium, "UDIMET 500"	47
Alloy Nickel-Cobalt-Chromium, "NIMONIC 105"	46
Alloy Nickel-Cobalt-Chromium, "IN-100", cast	46
Molybdenum, Commercial purity	46
Alloy Nickel-Chromium-Cobalt, "IN-162", cast	45
Alloy nickel-chromium, Inconel 713C, cast	45
Alloy Nickel-Cobalt-Chromium, "B-1900", cast	45

Figure 25 : Selection of constitutive materials according to the index M_2.

The materials proposed in this selection will have in addition to resist aggressive environmental conditions. Pure Molybdenum would be excluded, and most of Nickel alloys would require surface treatments, well developed in engine industries, to sustain these very demanding conditions. Beryllium alloys are possible solutions which are unlikely to be selected, since they are very difficult to use due to the health issues.

The processing of the material, in particular the fabrication of the spheres is also a limiting factor. Currently the spheres are obtained via electrodes positioned on polymer spheres. The optimal value for e/R is 0.016 which is 5 times smaller than the minimum thickness attainable in a reliable manner using this technique, which is 40µm. If this limitation is not removed in new processes, the choice

will be the alloy with the lowest density, namely the alloy IN-100. The fabrication of the necks is also an issue. Brazing seems a possible solution, and Ni alloys are easy to braze using Ni-Phosphorus. The technology would be then to process on the spheres a layer of brazing materials.

5 – SPECIAL COMMENTS ON MATERIALS BY DESIGN

We have proposed an example of "materials by design" for multifunctionnal requirements. The case studied concerns materials presenting simultaneously acoustic absorption properties and structural properties. The material investigated pertains to the class of hybrid materials for which both the constitutive material and the internal architecture are degrees of freedom for optimization. The procedure we have illustrated here combines quantitative modelling of acoustic and mechanical properties, performance analysis, and use of structured databases for material selection. The described method is to be seen as an illustration of a promising approach for multifunctionnal materials development.

6 – CONCLUSIONS AND IMPLICATIONS FOR FURTHER RESEARCH

During this three year contract we have successfully developed predictive tools describing the behaviour of Hollow Spheres based cellular materials. Properties such as acoustic absorption at normal temperature and under a thermal gradient, elasticity and macroscopic yielding as well as creep were handled by modelling and experiment for regular packing (Face Cubic Centred) of the hollow spheres based material. Progress in processing HS structures was also made.

These predictive tools were used in a "materials by Design" approach to establish concurrent tools and issues for optimized design of structures including this type of material. This approach was tested on a simple virtual design application and the principle was efficiently proved.

The obtained results demonstrate the promising performances of HS based cellular materials. Using these results and with appropriate processing improvements and developments, a good multidisciplinary research team could accelerate the industrial use of this promising multifunctional class of materials.

Nevertheless, an important effort will be required in the field of the cost reduction. The study of non regular packing of HS structures and the influence of the defaults presence inside regular packed structures on the properties of the material will become the main issue.

The research for generalised tools must be oriented for their use on enhanced and reliable properties predictability. The following topics will need further investigations for the non regular HS structures: acoustic and static mechanics, dynamics, thermal behaviour, damage evolution, fatigue, creep, oxidation and coupled acoustics with aerodynamics.

Industry is facing more and more multifunctional requirements related to several different aspects such as increasing performance, safety, comfort and reducing weight and cost. These "new type" of multifunctional structures will impose the use of multifunctional materials solutions or systems. The "Materials by design" approach, together with the enumerated predictive tools could be one of the best ways to respond to these stringent, necessarily multifunctional solutions.

FEVRIER 2005

7 – SUMMARY OF NOTEWORTHY INFORMATION DERIVED FROM OUR VARIOUS VISITS AND MEETINGS

* S. Gasser has attended "Metallic Composites and Foams Conference", 26-27 Nov. 2001, London, where he discussed the mechanical behavior of metallic foams with many specialists. He learned most pertinently investigation approaches such as those of Ashby and learned the need for accurate FEM calculations.

* S. Gasser and F. Paun have visited the Acoustic laboratory of Maine University, Le Mans, France December 2001, where they discussed the acoustic absorption in porous media with Y. Auregan and D. Lafarge (former students of Prof. Allard). The application of homogenization theory was analyzed.

* F. Paun has participated at the meeting of the "Foams and cellular materials research group", 21 May 2002, Lyon. *Note: This group gathers research scientists and industrial scientists from all over France in the above mentioned field.*

* S. Gasser has participated at the "Internoise 2002 Conference", 19-21 August 2002, Dearborn, Michigan, USA, where he presented a paper on the acoustic absorption under thermal gradient.

* S. Gasser and F. Paun have attended "BIOT Conference 2002", 26–28 August 2002, Grenoble, France where they discussed the acoustic absorption in porous media with many specialists and issues for a numerical implementation of the homogenization theory were analyzed.

* "Foams and cellular materials research group" meeting, December 16, 2002, Lyon, France.

  - S. Gasser presented a brief description of our research works,

  - Good feed-back from various scientists confirming the correct orientation of our project.

* Meeting with Prof. Mike Ashby in October 2002, Grenoble, France. F. Paun & S. Gasser discussed with Prof. Ashby about what they have discovered concerning the Young Modulus of hollow spheres based materials ; confirmation of the interest and the importance of these results by Mike Ashby.

* "Journée Scientifique de l'ONERA", January 16, Paris, France – "ONERA's Scientific Day" in the field of acoustic absorption materials organized at ONERA by F. Paun under T. Khan recommendation – details at www.onera.fr/congres/jso2003mat-bruit

* "Foams and cellular materials research group" meeting, June 6, 2003, Lyon, France.

* PhD Thesis presented by Stephane Gasser at ONERA on July 3, 2003, Paris, France
- Distinction and congratulations from the jury including Prof M. Ashby (University of Cambridge), Y. Brechet, J.L. Auriault (INPG, France), A. Mortensen (Ecole Polytechnique Lausanne, Switzerland), & Dr Y. Auregan (LAUM, France), H. Batard (AIRBUS, France), F. Paun (ONERA, France).
- Very appreciative referee's reports from A. Mortensen (mechanics) & Y. Auregan (acoustics)

* InterNoise 2003 Congress, August 2003, South Korea. Stephane Gasser presented our results on the acoustic absorption under thermal gradient.

* Euromat 2003 Congress, September 2003, Lausanne, Switzerland. Florin Paun presented our results on the elastic behavior of HS based cellular materials

* 20th AAAF Colloquium on Materials in Aerospace, 23-25 November, 2003, Paris, France

FEVRIER 2005

- Florin Paun organized the topic on acoustic absorptive materials as Organizing Committee member.
- Florin Paun had a keynote lecture on "Design of cellular materials for multifunctional applications"
- Yves Brechet had communication on "Lightweight materials design"

* "Foams and cellular materials research group" meeting, December, 2003, Lyon, France. Discussions with scientists concerning the local microplasticity in metallic foams ; possible influence on the macroscopic elastic behavior. The presence of porosity inside the cell walls or the brazing meniscus could induce direct macroscopic plastic behavior of the cellular material under any magnitude of mechanical loadings (lack of elasticity).

* Euromech 2004 Congres, 7-10 Juin, 2004, Nancy, France. Dr. Jason Nadler and Fady Mamoud presented their respective works on the Hollow Spheres based cellular material processing and modelling.

* Numiform 2004 Congres, 7-10 Juin, 2004, Columbus, OHIO, USA. Dr Florin Paun meat Dr Leo Christodoulou for brief scientific report on the present contract.

References

1] U.S. Patent N°-4,722,770 ; Blottiere & all, February 2, 1988

2] J-F. Alard, *Propagation of sound in porous media*, Elsevier Applied Science (1993)

3] M. R. Stinson, *"On acoustical models for sound propagation in rigid frame porous materials and the influence of shape factors"*, J. Acoust. Soc. Am. 92 (1992) p.1120

5] *PhD Thesis*, S. Gasser, INPG, France, 2003.

7] Denis Lafarge, Pavel Lemarinier, Jean F. Allard, Vigo Tarnow,*Dynamic compressibility of air in porous structures at audible frequencies*, Journal of Acoustical Society of America 102 (4), October 1997.

10] L.J. Gibson, M.F. Ashby, *Cellular Solids - Structure and Properties*, 2nd edition, Cambridge University Press, Cambridge, UK (1997)

12] W.S. Sanders, L.J. Gibson, *"Mechanics of BCC and FCC hollow-sphere foams", Mat. Sci. Engng. A* **352**, 150-161 (2003)

13] TJ Lim, B Smith, DL McDowel, "*Behavior of a random hollow sphere metal foam*", Acta Materialia, 50, 2867-2879 (2002)

15] U. Hornung, *Homogenization in porous media*, Springer-Verlag (1997)

16] S. Torquato, *Random heterogeneous materials*, Springer-Verlag (2002)

17] V.S. Deshpande, N.A. Fleck, J. Mech. Phys. Solids **48** ,1253-1283 (2000)

19] Ashby, M.F. (1999) "*Materials Selection in Mechanical Design*", 2nd edition, Butterworth Heinemann, Oxford UK.

20] Bréchet, Y., Ashby, M.F. and Salvo, L. (2001), "*Sélection des Matériaux et des Procédés de Mise en Oeuvre*", Presses Polytechniques et Universitaires Romandes de Lausanne, Switzerland (2001) (Volume 20 of the Series Traité des Matériaux)

21] ASM (1997), ASM Handbook Volume 20: "*Materials Selection and Design*", ASM International, Metals Park, Ohio, USA

22] Brechet Y., Bassetti D., Landru D., Salvo L.,(2001) Prog.Mat.Science, 46, 3-4, 407.

23] Ashby, M.F., Bréchet, Y.J.M., Cebon,D., Salvo,L. , (2003) *Materials and design*, (under press).

FEVRIER 2005

24] Bassetti D., Brechet Y., Heiberg G., Lingorski I., Pechambert P. and Salvo L., (1998), Proc. Conf. "*Composite Design for Performance*", Lake Louise, (P.Nicholson ed.), p. 88.

25] Deocon J., Salvo L., Lemoine P., Landru D., Brechet Y. and Leriche R., (1999) in *Metal Foams and Porous Metals Structures* (J.Banhardt, M.F.Ashby, N.A.Fleck eds.), MIT Verlag publishing, p. 325.

26] Duratti,L., Salvo,L., Brechet,Y. (2002) Advanced Engineering Materials, 4, 6, 367

27] CES4 (2002), *The Cambridge Engineering Selector*, Granta Design, Rustat House, 62 Clifton Road, Cambridge, CB17EG, UK (www.grantadesign.com)

FEVRIER 2005

Papers and articles published as a result of DARPA sponsored research.

4] Florin Paun, Stéphane Gasser, Laurent Leylekian, *Design of materials for noise reduction in aircraft engines*, (2003), Aerospace Sc.Tech.7, 1, 63

6] Stéphane Gasser, Florin Paun, Yves Bréchet, *Absorptive properties of rigid porous media: application to FCC sphere packing*, JASA, 2005 (under press)

8] S. Gasser, F. Paun, Y. Brechet, *Experimental investigation of acoustic absorption of a porous rigid material experiencing a high thermal gradient*, InterNoise Congress, September 2003, South Korea.

9] S. Gasser, F. Paun, Y. Brechet, *Influence of high temperature gradient on acoustic liners : Beyond the multilayer approach*, Internoise 2002, 19-21 August, Dearborn, Michigan, USA

11] Stephane Gasser, Florin Paun, Alexandre Cayzeele and Yves Brechet, *Uniaxial tensile elastic properties of a regular stacking of brazed hollow spheres*, Scripta Mat 2003, 48,12 , 1617

14] S. Gasser, F. Paun and Y. Bréchet, *Finite elements computation for the elastic properties of a regular stacking of hollow spheres*, Materials Science and Engineering A, Volume 379, Issues 1-2, 15 August 2004, Pages 240-244

18] S. Gasser, F. Paun, L. Riffard, Y. Brechet, *Microplastic yield condition for a periodic stacking of hollow spheres*, Scripta Materialia 50 (2004), 401-405, Elsevier

L'ONERA est le premier établissement de recherche français dans le domaine aéronautique et spatial, où il a pour mission de développer et d'orienter les recherches

L'ONERA est un organisme pluridisciplinaire qui décline ses projets de la recherche amont à leur aboutissement industriel. Ses « ingénieurs du ciel » imaginent, testent, simulent, modélisent et expérimentent les concepts nouveaux qu'ils livrent à l'industrie.

Depuis 50 ans au service de l'industrie aérospatiale civile et de défense

Les avions Airbus, Concorde, Mirage, Rafale ; les missiles Apache, ASMP et les lanceurs spatiaux Ariane ont bénéficié des travaux de l'ONERA.

Les clients et partenaires : Aerospatiale, CNES, DASA, Dassault, DGA, Matra Bae Dynamics, SNECMA, Thomson, etc. ainsi que les PME/PMI contribuent, au travers des projets menés en commun, à l'excellence scientifique et technique de l'ONERA.

Un nouvel élan pour un nouvel ONERA

Avec une organisation nouvelle, l'ONERA s'ouvre et s'adapte aux nouveaux besoins de l'industrie aéronautique et spatiale.
Les Grands Moyens Techniques regroupant ingénierie et bureaux d'études, les grands moyens de calcul et un parc de souffleries unique en Europe, apportent une assistance technique de haut niveau à une clientèle internationale.

Dix huit départements spécialisés sont répartis dans quatre branches scientifiques : Mécanique des fluides et énergétique, Physique, Matériaux et structures, Traitement de l'information et systèmes.

French aerospace research agency ONERA sets strategic research objectives and supports the development of research initiatives.

ONERA is a multidisciplinary organization, conducting upstream research projects that lead to industrial applications. Our scientists, engineers and technicians conceive, simulate, model and test solutions, which are then delivered to industry.

50 years at the cutting edge of civil and military aerospace research

ONERA has been involved in the development of a number of landmark aerospace projects, from the Airbus and Concorde jetliners, to Mirage and Rafale fighters, Apache and ASMP missiles and Ariane launch vehicles.
Our partners and customers include Aerospatiale, CNES (French space agency), DASA, Dassault, DGA (French arms-procurement agency), Matra BAe Dynamics, SNECMA and Thomson-CSF. We also team up with smaller companies on joint projects that have helped build Onera's reputation for scientific and technical excellence.

A revamped ONERA steps up the pace

ONERA has revamped its structures to keep pace with the fast-changing requirements of the aerospace industry.
We have set up a Technical Resources Division, grouping our design and engineering teams, large-scale computation facilities and an array of wind tunnels unique in Europe. By consolidating these resources in a single division, we can provide the high-level technical assistance demanded by customers from around the world.
ONERA has also set up four major scientific groups Fluid Mechanics and Energetics, Physics, Materials and Structures, Information Technology and Systems which are organized in 18 departments, each enjoying a wide degree of operational independence.

Office National d'Études et de Recherches Aérospatiales
BP 72 - 29 avenue de la Division Leclerc
92322 CHATILLON CEDEX
Tél. : +33 1 46 73 40 40 - Fax : +33 1 46 73 41 41
http://www.onera.fr